

Supporting information

Inherently Magnetic Hydrogel for Data Storage Based on Magneto-Optical Kerr Effect

By *Qinyuan Gui, You Zhou, Shenglong Liao, Yonglin He, Yifan Tang and Yapei Wang**

Table of Contents

1. Supporting Note S1: Materials
2. Supporting Note S2: Experimental section
3. Supporting Note S3: Decrease in Young modulus with the increasing concentration of $\text{Dy}(\text{OH})_3$
4. Supporting Note S4: Thermogravimetric analysis (TGA)
5. Supporting Note S5: Abnormal phenomenon in the hysteresis loop of PAAm hydrogel
6. Supporting Note S6: Brief introduction to the mechanism of Magneto-Optical Kerr Effect (MOKE)
7. Data section

1. Supporting Note S1: Materials

Sodium alginate (AR) and ammonium persulphate (APS, AR) were purchased from Lyntech, Beijing, China. Acrylamide (AM, 99%), D-glucono- δ -lactone (GDL, 99%) and sodium hydroxide (NaOH, 96%) were purchased from Aladdin, Shanghai, China. The dysprosium oxide (Dy_2O_3 , 99.99%) was provided by Energy Chemical, China. N,N'-methylenebisacrylamide (MBAA, 97%) was obtained from Alfa Aesar. N,N,N',N'-tetramethylethylenediamine (TEMED, 99%) was supplied by J&K Scientific. Perchloric acid (HClO_4 , 70-72%) was provided by Tianjin Xinyuan Chemical Co., LTD., China.

2. Supporting Note S2: Experimental Section

(1) Preparation of dysprosium hydroxide

The dysprosium hydroxide ($\text{Dy}(\text{OH})_3$) was prepared with the Dy_2O_3 as Dy^{3+} supplier. The Dy_2O_3 was first put into a HClO_4 solution (0.2 M) and stirred under 40 °C until the Dy_2O_3 was fully dissolved. The concentration of HClO_4 solution was relatively low to prevent explosion under heating and stirring. Subsequently, excessive amount of NaOH was added to the $\text{Dy}(\text{ClO}_4)_3$ solution to eliminate residual HClO_4 and form $\text{Dy}(\text{OH})_3$ precipitate. Then, the $\text{Dy}(\text{OH})_3$ was repeatedly washed by water and centrifuged for 10 times to ensure the complete removal of remanent NaOH. Finally, the $\text{Dy}(\text{OH})_3$ was freeze-dried under vacuum and sealed in glass bottle for later use.

(2) Preparation of inherent magnetic DN hydrogel

The DN hydrogel was synthesized by mixing two types of crosslinked hydrogels. The acrylamide was first dissolved in deionized water with a mass fraction of 20%. Subsequently, $\text{Dy}(\text{OH})_3$ powder was added into the solution and sonicated until it was completely dispersed. The amount of $\text{Dy}(\text{OH})_3$ was determined by the ratio between Dy^{3+} and $-\text{COO}^-$. Then, APS and MBAA with the mass fraction of 0.1% and 0.01%, respectively, were dissolved into the mixture. After that, 2 wt.% of sodium alginate

was added into the mixture and stirred overnight. It is noteworthy that stirring should be conducted in dark under cool environment to prevent the acrylamide from crosslinking.

After adequate stirring, GDL was added into the mixture to act as the Dy^{3+} initiator. The molar ratio of GDL was 4 times higher than that of $\text{Dy}(\text{OH})_3$ to guarantee the $\text{Dy}(\text{OH})_3$ powder was fully resolved. Different from CaCO_3 , the reaction between gluconic acid and $\text{Dy}(\text{OH})_3$ was much slower, which affords enough time for the later operation. Subsequently, TEMED, the amount of which was determined by the molar ratio with GDL, was dissolved into the system. The hydrogel was cured within 2 min after the fully dispersion of TEMED and the resulting hydrogel was turbid and in light yellow (Figure S1a). However, the hydrogel became transparent after sealed and placed under room temperature for one week, owing to the complete reaction of $\text{Dy}(\text{OH})_3$ (Figure S1b). The DN hydrogel was able to be attracted by the magnet as shown in **Figure S2**.

(3) Rheological test of the DN hydrogel

The hydrogel sample was fabricated as a square shape with a thickness of 1 mm and then cut into a round plate with a diameter of 8 mm for rheological test, which was carried through a rheometer (TA ARES-G2). To measure the linear viscoelastic region, the experiment was carried out at different strains ranging from 0.01 to 100 % with the temperature fixed at 25 °C. Then the storage modulus (G') and loss modulus (G'') were assessed by applying a constant strain (0.1 %) within the linear viscoelastic region over a frequency range from 100 to 0.01 Hz.

(4) Mechanical property measurement of the DN hydrogel

The tensile test was conducted by the Instron 5943 universal machine with a 5 N load cell under room temperature. For both extension test and cycle test, the loading speed was fixed at 100 mm/min. Before the test, the samples were modeled into dog-bone shape to ensure the break occurs in the certain region of the sample.

(5) Magnetic property measurement

Magnetic property measurement was carried on the Quantum Design PPMS-9 which is a physical property measurement system. Considering the experiment was conducted under vacuum and may have some vibration during the test, all samples were freeze-dried before the experiment to avoid the water evaporation induced baseline drift. The hysteresis loop measurement was conducted under 300 K while the magnetic field swept from -3 T to 3 T. When the magnetic field was lower than 5000 Oe, the sweeping speed was fixed at 50 Oe/s, and the speed rose to 150 Oe/s when the magnetic field was above 1 T. The low-temperature hysteresis loop was conducted under the same condition except for the magnetic field was ranging from -5 T to 5 T. In the Curie temperature measurement, the magnetic field was fixed at 100 Oe while the temperature reduced from 300 K to 2 K. Above 10 K, the speed of temperature reduction was 10 K/min. However, under 10 K, the temperature reduction speed was reduced to 1 K/min, which was the limitation of the apparatus.

(6) MOKE test for data storage experiment

The samples were streakily patterned with different magnetic properties by time-resolved selective bonding of Ca^{2+} and Dy^{3+} with alginate (Figure 4b). The experiment was conducted on NanoMOKE3 (Durham) which is a magneto-optical Kerr measurement system. To obtain the largest polar MOKE signal, the angle of incident light and reflected light were both 90° with the magnetic field perpendicular to the sample. To visually distinguish the magnetic property induced difference in rotation of plane of polarization, which was illustrated by the brightness of stripes, a mapping mode was applied with a magnification of 286 times. During the experiment, the magnetic field swept from -1000 Oe to 1000 Oe and a picture was exported every 120 Oe. By setting a picture at low field as the substrate, the contrast between Dy^{3+} and Ca^{2+} becomes more obvious at high magnetic field, thus realizing the data storage.

3. Supporting Note S3: Decrease in Young modulus with the increasing concentration of $\text{Dy}(\text{OH})_3$

We prepared three hydrogels with various ratios between $-\text{COO}^-$ and Dy^{3+} of 4:1, 2:1 and 1:1, respectively. As illustrated in Figure S4a, the slope of the elastic stage decreases upon increasing concentration of Dy^{3+} . Figure S4b presents the Young modulus calculated from Figure S4a. Specifically, the modulus decreases from 21.70 kPa to 0.76 kPa with the ratio increases from 4:1 to 1:1.

Here, we raise an assumption to explain the above phenomenon. The alginate hydrogel in our system is not crosslinked immediately. The Dy^{3+} was formulated by the reaction between hydrolyzed D-glucono- δ -lactone (GDL) with $\text{Dy}(\text{OH})_3$. To ensure the $\text{Dy}(\text{OH})_3$ was completely decomposed, the GDL was added excessively. Therefore, the whole system is acidic. If the ratio between $\text{Dy}(\text{OH})_3$ and GDL is controlled as 1:4, then increasing the concentration of $\text{Dy}(\text{OH})_3$ will lead to more GDL, thus resulting in more residual GDL after the reaction. The increased amount of residual GDL will decrease the pH of the whole system dramatically, which is a possible origin of the difference between our system and the others.

4. Supporting Note S3: Thermogravimetric analysis (TGA)

To confirm the alginate hydrogel and PAAm hydrogel were coupled with each other, the thermal decomposition experiment was conducted on alginate, PAAm, and DN hydrogel. The TGA was performed on a Q500 TGA (TA Instruments) under the nitrogen atmosphere with flow rate of 40 mL/min. Samples were loaded on platinum pans and ramped to 900 °C at a rate of 10 °C/min.¹ Before the test, the samples were lyophilized in vacuum to prevent the interference from water. The original TGA data was illustrated in **Figure S5a** and the differential thermogravimetric data (DTG) was demonstrated in Figure S5b. The DTG was obtained by the derivative of the weight loss percentage with respect to the time from the TGA data.

As shown in Figure S5a, the degradation curve of each hydrogel different from each other. Among all three hydrogels, the alginate hydrogel possesses the highest percentage amount of residual while the PAAm shows the lowest. This notable difference was because the Dy^{3+} -alginate hydrogel generates Dy_2O_3 at high

temperature while the PAAm generates mostly CO₂ and H₂O. To the DN hydrogel, labeled as hybrid in Figure S5, the amount of residual was between the alginate hydrogel and PAAm hydrogel.

The critical evidence to prove the formation of double network was provided in Figure S5b. Each peak on the DTG curve indicates the pyrolysis occurs in a reasonable temperature range. As illustrated in Figure S5b, two high peaks, at the range of 307-400 °C and 600-750 °C respectively, and one small peak at the range of 250-300 °C were appeared on the PAAm curve. For the alginate curve, four main curves ranged in 180-240 °C, 240-300 °C, 300-480 °C, and 480-730 °C were observed. The peak in the range of 240-300 °C was attributed to the degradation of carboxyl group and the peak at the 480-730 °C was a result of depolymerization of the hydrogel and the formation of Dy(OH)₃. Interestingly, when it comes to the DN hydrogel, the number of peaks was not the simple sum of the individual materials. The quantity reduction and location shift of peaks on the hybrid curve was a direct evidence to the formation of new chemical bond. In other words, the alginate and PAAm were covalently coupled.²

5. Supporting Note S4: Abnormal phenomenon in the hysteresis loop of PAAm hydrogel

An interesting phenomenon comes up with the PAAm single network hydrogel. In Figure S6, the slope of the hysteresis loop of PAAm hydrogel is positive within the range of low magnetic field, which disagrees with its diamagnetic property. Additionally, below the Curie temperature, the susceptibility of the PAAm is positive under the magnetic field of 100 Oe (Figure S7). It is assumed that this abnormal character is caused by the shape magnetic anisotropy, which may occur when the geometrical shape of the sample is irregular even in a uniform system. This phenomenon was surpassed in the other hydrogel samples due to the strong paramagnetic signal of Dy³⁺ ions.

6. Supporting Note S5: Brief introduction to the mechanism of Magneto-Optical

Kerr Effect (MOKE)

Controversy exists when it comes to the mechanism of MOKE. Up to now, two theories are generally accepted, including the microtheory and the macrotheory. Each will be discussed in detail in the following.³

(1) Microtheory

In the microtheory, MOKE results from the interaction between the radiation field and the electron. Therefore, the theory inevitably applies the equation of electronic motion, the Maxwell equation, and the Fresnel's reflection matrix. It is noteworthy that the reflected light is interconnected with the transmission light. In other words, the reflected light is a result of the transmission field. In this regard, the refractive index is also of great importance in consideration of MOKE.

Considering a beam travelling from medium 1 to medium 2. The incident angle is θ_1 and the refraction angle is θ_2 . Let us assume p and s as the parallel and perpendicular components of the field, i and r as the incident and reflected light, E as the electric field, respectively. So the reflective matrix can be written as:

$$\begin{bmatrix} E_s^r \\ E_p^r \end{bmatrix} = \begin{bmatrix} r_{11} & r_{12} \\ r_{21} & r_{22} \end{bmatrix} \begin{bmatrix} E_s^i \\ E_p^i \end{bmatrix} \quad (1)$$

where

$$\left. \begin{aligned} r_{11} &= \frac{n_1^2 \cos^2 \theta_1 - n_{2+} n_{2-} \cos^2 \theta_2}{(n_1 \cos \theta_1 + n_{2+} \cos \theta_2)(n_1 \cos \theta_1 + n_{2-} \cos \theta_2)} \\ r_{12} &= i \frac{n_1 \cos \theta_1 \cos \theta_2 (n_{2-} - n_{2+})}{(n_1 \cos \theta_2 + n_{2+} \cos \theta_1)(n_1 \cos \theta_2 + n_{2-} \cos \theta_1)} \\ r_{21} &= i \frac{n_1 \cos \theta_1 \cos \theta_2 (n_{2-} - n_{2+})}{(n_1 \cos \theta_1 + n_{2+} \cos \theta_2)(n_1 \cos \theta_1 + n_{2-} \cos \theta_2)} \\ r_{22} &= \frac{n_1^2 \cos^2 \theta_2 - n_{2+} n_{2-} \cos^2 \theta_1}{(n_1 \cos \theta_2 + n_{2+} \cos \theta_1)(n_1 \cos \theta_2 + n_{2-} \cos \theta_1)} \end{aligned} \right\} (2)$$

In the equation (2), the n_1 represents for the refractive index of medium 1 while n_2 represents the refractive index of medium 2. However, when the light enters the medium 2, the right- and left-hand circularly polarized light are differentiated. To distinguish each other, we use n_{2+} to represent the refractive index of right-hand circularly polarized light and n_{2-} to represent the refractive index of left-hand circularly polarized light. Considering the light is a vertical incidence with $E_p^i = 0$,

which is easy to realize. Moreover, normally, the medium 1 is air, which means $n_1 = 1$.

In this case, the equation (1) and (2) can be simplified as:

$$\begin{aligned} \begin{bmatrix} E_s^r \\ E_p^r \end{bmatrix} &= \begin{bmatrix} r_{11} & r_{12} \\ r_{21} & r_{22} \end{bmatrix} \begin{bmatrix} E_s^i \\ 0 \end{bmatrix} \quad (3) \\ \left. \begin{aligned} r_{11} = r_{22} &= \frac{1 - n_{2+} + n_{2-}}{(1 + n_{2+})(1 + n_{2-})} \\ r_{12} = r_{21} &= i \frac{n_{2-} - n_{2+}}{(1 + n_{2+})(1 + n_{2-})} \end{aligned} \right\} \quad (4) \end{aligned}$$

If assuming the Kerr rotation angle as θ_k , according to geometry, it is easy to conclude that

$$\tan \theta_k = -\frac{E_p^r}{E_s^r} = -\frac{r_{21}}{r_{11}} = -i \frac{n_{2+} - n_{2-}}{n_{2+} + n_{2-} - 1} \quad (5)$$

In practical experiment, the θ_k is very small, so $\tan \theta_k$ can be approximated to θ_k . Moreover, the interaction between light and medium 2 is inevitable. Taking this interaction into consideration, the refraction index should be expressed as

$$n_{\pm} = N_{\pm} - iK_{\pm} \quad (6)$$

Here, because the refraction index is a determined value, we use n_{\pm} to replace $n_{2\pm}$.

Applying equation (6) to equation (5), let

$$\left. \begin{aligned} N_+ - N_- = \Delta N, \quad K_+ - K_- = \Delta K \\ N = \frac{1}{2}(N_+ + N_-), \quad K = \frac{1}{2}(K_+ + K_-) \end{aligned} \right\} \quad (7)$$

Then, the equation (5) can be transformed into

$$\theta_k = \frac{2NK\Delta N - \Delta K(N^2 - K^2 - 1)}{(N^2 - K^2 - 1)^2 + 4N^2K^2} + i \frac{2NK\Delta N + \Delta N(N^2 - K^2 - 1)}{(N^2 - K^2 - 1) + 4N^2K^2} \quad (8)$$

To figure out n_+ and n_- , we should first consider the equation of electronic motion

$$m\ddot{r} = -m\omega_0^2 r + e \left(E + \frac{1}{3\epsilon_0} P \right) - g\dot{r} + e\mu_0 H_i \dot{r} \times k \quad (9)$$

where ω_0 is the angular frequency of the electronic motion, m and e are electronic mass and charge, respectively. E represents the electric field and $P = N_0 e r$ the electric polarization vector. ϵ_0 stands for the permittivity of vacuum. N_0 is the number density of the electron. H_i stands for the effective field and k is the unit vector. The first term on the right side refers to the centripetal force given by the positive center to the electron. The second term is the force given by local electric field. The third term

represents the damping force caused by the accelerate movement of the electron. The forth term is the interaction between effective field and the electron. Taking both equation 6 and Maxwell equation into consideration, the refraction index of right- and left-hand polarized light can be written as,

$$\left. \begin{aligned} n_+^2 - 1 &= \frac{\frac{\mu_0 N_0 e^2 c^2}{m}}{\omega_0^2 - \omega^2 - i\gamma\omega - \frac{Ne^2}{3\varepsilon_0 m} + \frac{e\mu_0 \omega H_i}{m}} \\ n_-^2 - 1 &= \frac{\frac{\mu_0 N_0 e^2 c^2}{m}}{\omega_0^2 - \omega^2 - i\gamma\omega - \frac{Ne^2}{3\varepsilon_0 m} - \frac{e\mu_0 \omega H_i}{m}} \end{aligned} \right\} (10)$$

where c is the light speed in the vacuum and ω is the circular frequency of light. $\gamma = \frac{g}{m}$ is a constant. So far, the only unknown parameter is the effective field H_i , and the expression of H_i can be written as

$$H_i = H_e + H_d + H_\lambda + H_v + \dots (11)$$

where H_e is the external magnetic field. H_d is the demagnetizing field. H_λ is the effective field related to the anisotropy. H_v is the spin-orbit interaction related to effective field which is intensely connected to the magnetic property of the sample.

(2) Macrotheory

The macrotheory is established on the tensor theory. The root of optical property of the matter is the dielectric property. In other words, the change of optical property is a representation of the change in dielectric property. Physically speaking, the nature of the dielectric property is a matrix which can be written as a second order tensor,

$$\varepsilon = \begin{pmatrix} \varepsilon_{xx} & \varepsilon_{xy} & \varepsilon_{xz} \\ \varepsilon_{yx} & \varepsilon_{yy} & \varepsilon_{yz} \\ \varepsilon_{zx} & \varepsilon_{zy} & \varepsilon_{zz} \end{pmatrix} (12)$$

Thus, when the sample is placed in the magnetic field, the magnetic moment will be reoriented to a new direction depending on the magnetic property, leading to the change of the dielectric tensor. This change in the element of dielectric tensor will eventually alter the optical property.

When light travels in the air, it obeys the Maxwell equation,

$$\left. \begin{aligned} \nabla \times H - \frac{\partial D}{\partial x} &= j \\ \nabla \times E + B &= 0 \\ \nabla \cdot D &= \rho \\ \nabla \cdot B &= 0 \end{aligned} \right\} (13)$$

where D is the electric displacement vector which can be expressed as,

$$D = \begin{pmatrix} D_x \\ D_y \\ D_z \end{pmatrix} = \varepsilon E = \begin{pmatrix} \varepsilon_{xx} & \varepsilon_{xy} & \varepsilon_{xz} \\ \varepsilon_{yx} & \varepsilon_{yy} & \varepsilon_{yz} \\ \varepsilon_{zx} & \varepsilon_{zy} & \varepsilon_{zz} \end{pmatrix} \begin{pmatrix} E_x \\ E_y \\ E_z \end{pmatrix} (14)$$

Combining both equation (13) and (14), we can get

$$\mu \varepsilon_k E_k = n^2 [E_k - s_k (E \cdot s)], (k = x, y, z) (15)$$

where n is the refractive index. s_k is the direction component of the light. s is the unit vector of the light. To make equation (15) meaningful, the refraction index, the propagation direction and the dielectric constant should obey the Fresnel equation. In that case, if the dielectric constant is confirmed, the relationship between refraction index and polarization state of the light can be well expressed.

Imagining a light travels from medium 1 to medium 2, with the magnetic field perpendicular to the sample pointing to the z direction. The incident plane lies in the y - z plane (**Figure S8**). At the interface of medium 1 and 2, the tangential component of the electric and magnetic field should be continuous. Here, a boundary matrix F is used to describe the tangential component and P is set to describe the electric field in the incident and reflected light,

$$F = \begin{pmatrix} E_x \\ E_y \\ H_x \\ H_y \end{pmatrix}, P = \begin{pmatrix} E_s^i \\ E_p^i \\ E_s^r \\ E_p^r \end{pmatrix} (16)$$

In our experiment, the DN hydrogel was placed on a piece of black abrasive paper. So when the light travels to the bottom of the sample, no reflection is supposed to occur owing to the light absorption. Consequently, we have to consider only one boundary condition. To transform matrix P into F , a 4×4 matrix was needed. Defining this 4×4 matrix as matrix A , the relationship of F , P and A should be correlated as,

$$F = AP (17)$$

In medium 1 and 2, the following equations are satisfied respectively,

$$F_1 = A_1 P_1, F_2 = A_2 P_2 (18)$$

Owing to the boundary condition, the tangential component should be equal to each other. In other words,

$$A_1 P_1 = A_2 P_2 \quad (19)$$

For the polar Kerr effect in medium 2, the matrix A_2 has the formation of

$$A_2 = \begin{pmatrix} 1 & 0 & 1 & 0 \\ \frac{i}{2}Q\sin^2\theta & \cos\theta & \frac{i}{2}Q\sin^2\theta & -\cos\theta \\ \frac{i}{2}QN\cos\theta & -N & -\frac{i}{2}QN\cos\theta & -N \\ N\cos\theta & \frac{i}{2}QN & -N\cos\theta & \frac{i}{2}QN \end{pmatrix} \quad (20)$$

where N is the refractive index of the medium before being magnetized and Q is the magneto-optical constant. θ is the refraction angle. If the polarization direction of incident light is perpendicular to the incident plane, the following physical quantity can be defined as eq.(21),

$$r_{ss} = \frac{E_{1s}^r}{E_{1s}^i}, r_{ps} = \frac{E_{1p}^r}{E_{1s}^i}, t_{ss} = \frac{E_{2s}^t}{E_{1s}^i}, t_{ps} = \frac{E_{2p}^t}{E_{1s}^i} \quad (21)$$

Where t in the superscript stands for the transmission light. Taking equation (21) into consideration, the equation (19) can be written as eq. (22),

$$A_1 \begin{pmatrix} 1 \\ 0 \\ r_{ss} \\ r_{ps} \end{pmatrix} = A_2 \begin{pmatrix} t_{ss} \\ t_{ps} \\ 0 \\ 0 \end{pmatrix} \quad (22)$$

Finally, after experimentally measuring Q and controlling the other conditions, the Kerr angle can be figured out through connecting all the equation above,

$$\theta_k = \frac{r_{ps}}{r_{ss}} \quad (23)$$

7. Data section

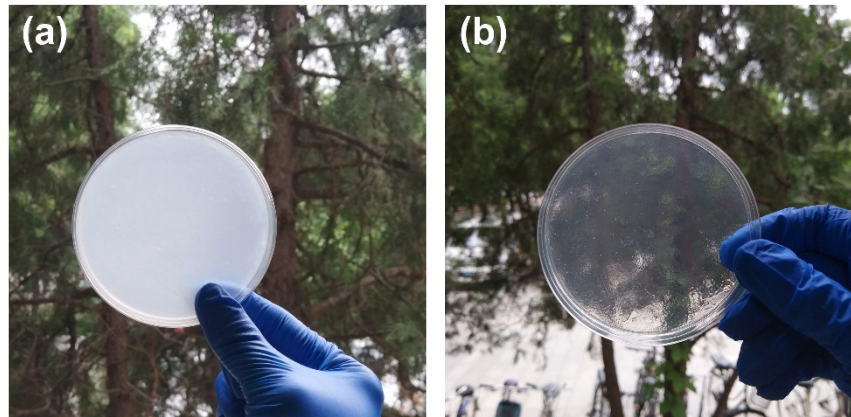


Figure S1. (a) The just-fabricated double network hydrogel was cloudy owing to the $\text{Dy}(\text{OH})_3$ powder suspended in it. It is not possible to see through the hydrogel to vision the tree on the other side. (b) After 1 week of preservation, the DN hydrogel becomes transparent. Through the hydrogel, we can see the tree on the other side. This is because the GDL released completely and the $\text{Dy}(\text{OH})_3$ was fully degraded.

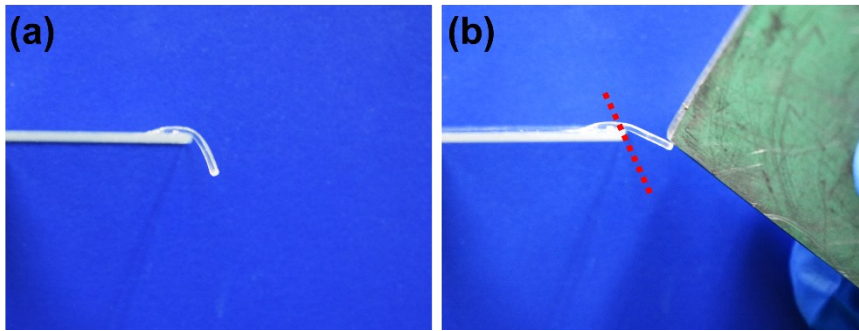


Figure S2. (a) A magnetic DN hydrogel was cut into a slice with thickness of 1 mm and placed on a piece of glass without applying the external magnetic field. (b) A magnet was placed near the DN hydrogel and the hydrogel is attracted by the magnet. The red dashed line is the original state of the hydrogel.

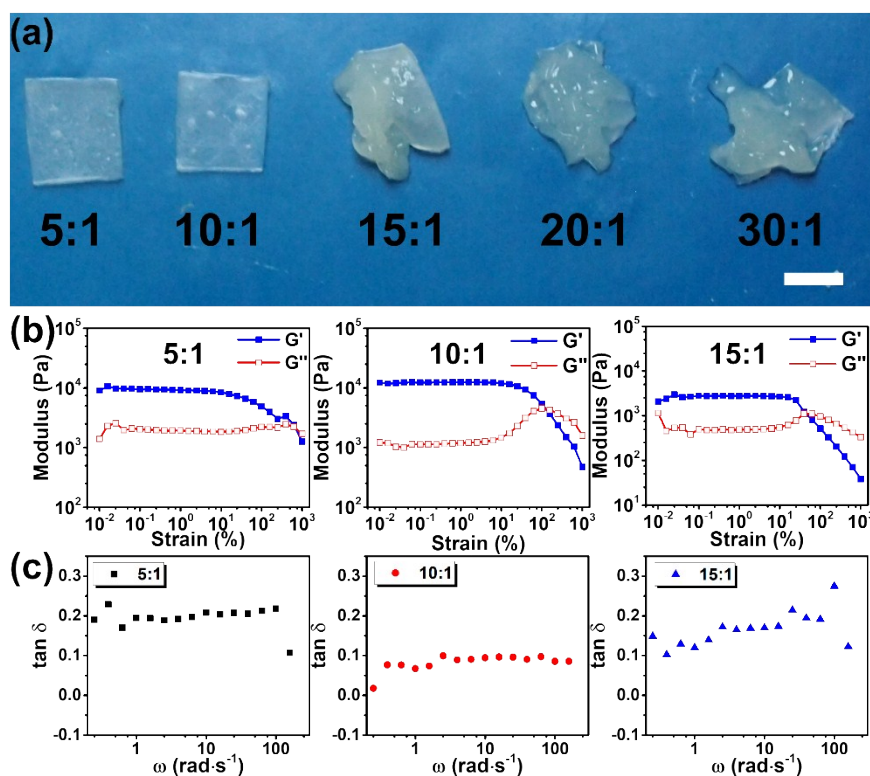


Figure S3. (a) Optical image of the DN hydrogels with different ratio of GDL:TEMED. The 5:1 and 10:1 samples are free-standing. The 15:1 sample is partially collapsed. The 20:1 and 30:1 samples exhibit pure liquid state. The scale bar in the figure is 1 cm. (b) The linear viscoelastic range of the DN hydrogels with the GDL:TEMED=5:1, 10:1 and 15:1. The 20:1 and 30:1 samples are excluded from the measurement owing to their liquid state. The blue cube stands for the storage modulus and the red hollow cube represents the dissipative modulus. (c) The loss tangent of the DN hydrogels with different parameters. All the tests are carried within the linear viscoelastic range.

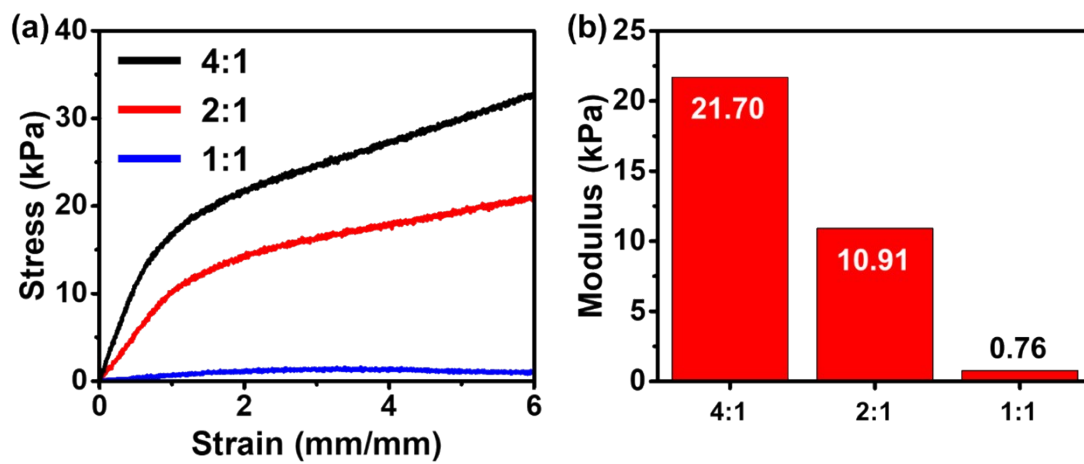


Figure S4. (a) Stress-strain curves of three hydrogels with various concentrations of Dy^{3+} . (b) Young modulus of the hydrogel with different concentrations of Dy^{3+} calculated from (a).

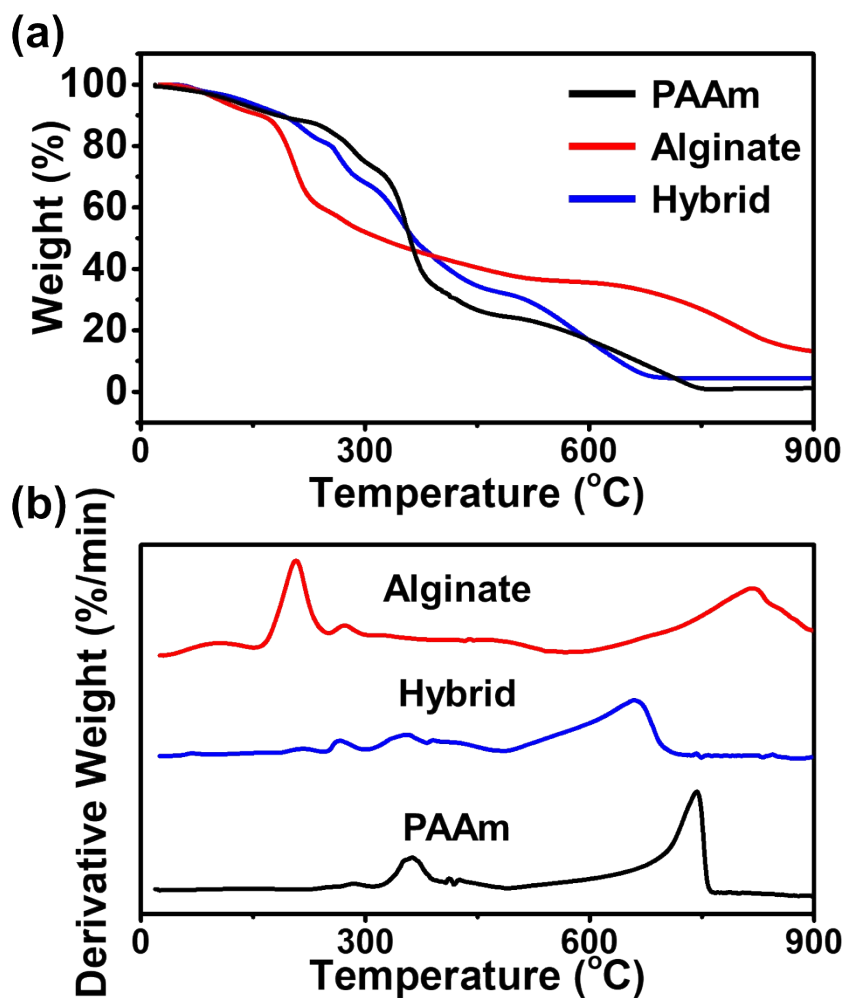


Figure S5. (a) Thermogravimetric analysis (TGA) tests on PAAm hydrogel, Dy³⁺-alginate hydrogel, and DN hydrogel. For simplicity, the DN hydrogel is labeled as Hybrid in the figure. (b) Differential thermogravimetry (DTG) data of three types of hydrogels.

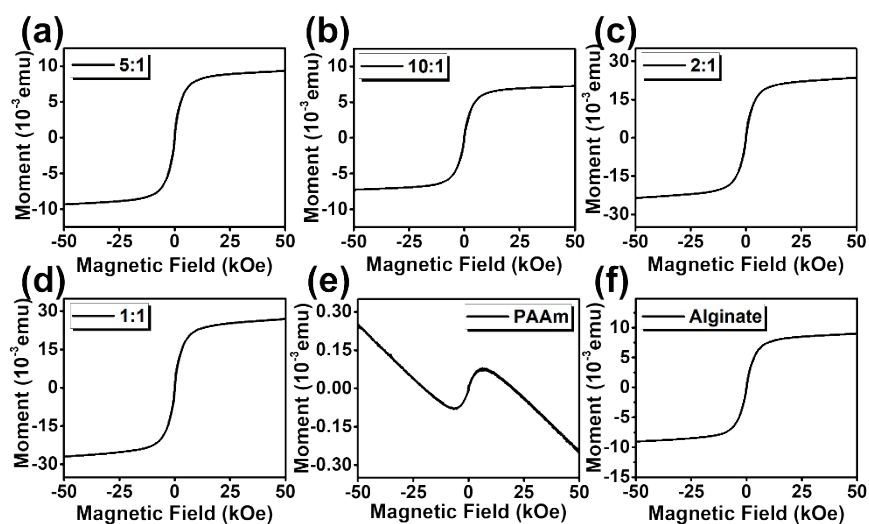


Figure S6. The hysteresis loop of the hydrogels with different parameters. **(a)** GDL:TEMED=5:1 while the Dy^{3+} :- COO^- =1:4. **(b)** GDL:TEMED=10:1 while the Dy^{3+} :- COO^- =1:4. **(c)** GDL:TEMED=10:1 while the Dy^{3+} :- COO^- =1:2. **(d)** GDL:TEMED=10:1 while the Dy^{3+} :- COO^- =1:1. **e.** PAAm single network hydrogel. **(f)** Dy^{3+} -alginate single network hydrogel.

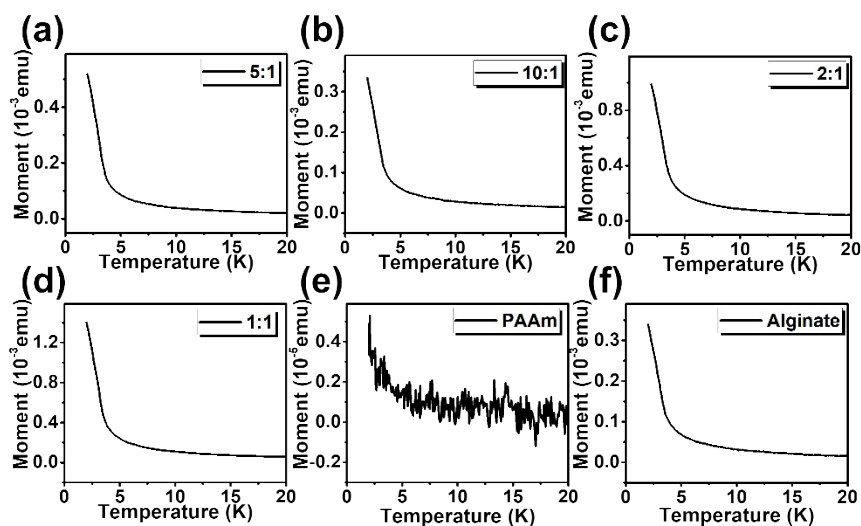


Figure S7. Magnetic susceptibility depends on the temperature, revealing the Curie temperature of different samples. **(a)** GDL:TEMED=5:1 while the Dy³⁺:-COO⁻=1:4. **(b)** GDL:TEMED=10:1 while the Dy³⁺:-COO⁻=1:4. **(c)** GDL:TEMED=10:1 while the Dy³⁺:-COO⁻=1:2. **(d)** GDL:TEMED=10:1 while the Dy³⁺:-COO⁻=1:1. **(e)** PAAm single network hydrogel. **(f)** Dy³⁺-alginate single network hydrogel.

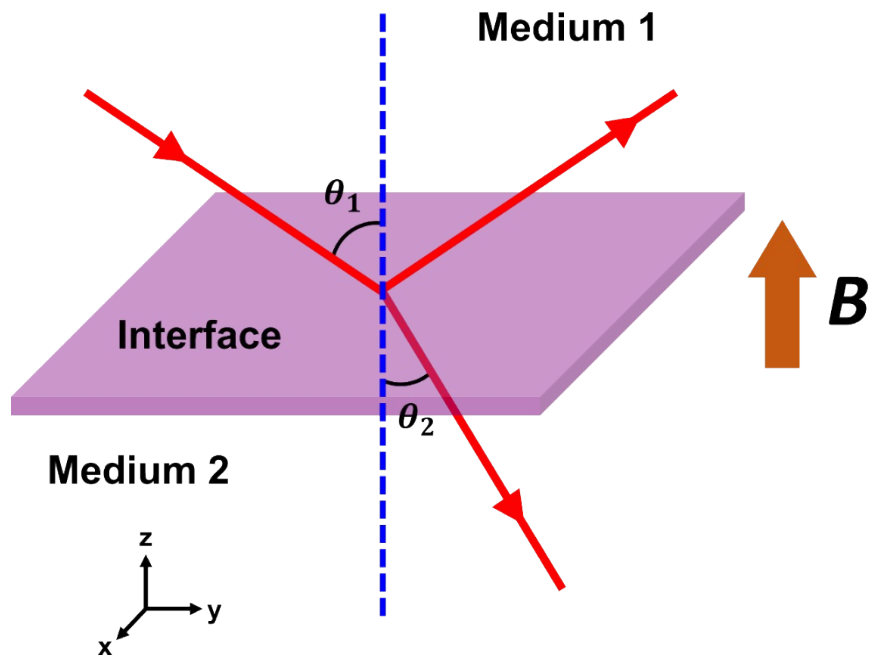


Figure S8. The scheme of optical path for convenient understanding of MOKE calculation. The red lines represent the path of the light and the red arrows indicate the direction of the light propagation. The blue dashed line serves as the normal and the brown arrow is the direction of the external magnetic field. θ_1 and θ_2 stand for the angle of incidence and refraction respectively.

References

- (S1) He, Y.; Gui, Q.; Wang, Y.; Wang, Z.; Liao, S.; Wang, Y., A Polypyrrole Elastomer Based on Confined Polymerization in a Host Polymer Network for Highly Stretchable Temperature and Strain Sensors. *Small* **2018**, *14*, 1800394(1)-1800394(2).
- (S2) Sun, J. Y.; Zhao, X.; Illeperuma, W. R.; Chaudhuri, O.; Oh, K. H.; Mooney, D. J.; Vlassak, J. J.; Suo, Z., Highly stretchable and tough hydrogels. *Nature* **2012**, *489*, 133-136.
- (S3) Zak, J.; Moog, E. R.; Liu, C.; Bader, S. D., Universal approach to magneto-optics. *J. Magn. Magn. Mater.* **1990**, *89*, 107-123.G